JOURNAL OF THERMOPHYSICS AND HEAT TRANSFER
Vol. 20, No. 3, July–September 2006

Technical Notes

TECHNICAL NOTES are short manuscripts describing new developments or important results of a preliminary nature. These Notes should not exceed 2500 words (where a figure or table counts as 200 words). Following informal review by the Editors, they may be published within a few months of the date of receipt. Style requirements are the same as for regular contributions (see inside back cover).

Profile Patterns and Stability of Evaporating Liquid Sessile Drops

David F. Chao* and John M. Sankovic*
NASA John H. Glenn Research Center at Lewis Field, Cleveland, Ohio 44135
and
Nengli Zhang†
Ohio Aerospace Institute, Cleveland, Ohio 44142

Nomenclature

b = drop protruding foot height, mm
f = space curved surface function of the initial wavefont
L = distance between the drop and the screen
P = point on the initial wave front
Q = inflexion point on the initial wave front
$\boldsymbol{R}$ = projective position on x–y coordinate plane of points in the wave front space
t = sessile drop spreading/evaporating time, s
t_f = lifetime of sessile drops, s
$t_{f'}$ = eigenlifetime, s
W = initial wave front produced by a liquid body reforming monochromatic plane wave of laser beam
Z = Cartesian coordinaate in vertical direction
θ = contact angle of a sessile drop
τ = dimensionless spreading/evaporating time of a sessile drop, identical to t/t_f
τ' = dimensionless spreading/evaporating eigentime of a sessile drop, identical to $t/t_{f'}$
Ω = observation space in far field of the wave

I. Introduction

THE study of spreading characteristics and spreading mechanisms deserves special attention. It is generally recognized that a precursor film and a protruding foot (crossover region between the bulk body of the drop and the precursor film) in the very edge of a liquid front, with typical thicknesses of order of 10 nm and 10 μm, respectively, strongly affect the spreading of liquids.[1–3] It is important to determine the behavior of the sessile drop near the three phase contact line (TPCL) region when the instant geometric parameters of the drop, such as contact diameter, contact angle, and volume, are measured.

Spreading of nonvolatile liquid drops has been well studied by many investigators for its simplicity in theoretical analysis. Zhang and Yang[4–6] and Zhang and Chao[7,8] performed a series of studies on spreading of volatile liquid sessile drops. Zhang and Yang[4] successfully used drop-refractive far-field shadowgraphy to study the interfacial stability in spreading and evaporating liquid drops. The spreading drops were classified into three types: stable, substable, and unstable interface. Chao and Zhang[9] further discovered that both evaporation and thermocapillary convection strongly affect the drop spreading and contact angle. An optical method has been developed by Zhang and Chao[10,11] and Chao et al.[12] to determine the profiles of sessile drop at the TPCL and to visualize capillary flow in the drop simultaneously. This study reveals various spreading profile patterns of evaporating sessile drops.

II. Principles of Method

When a parallel laser beam passes through a sessile drop on a slide glass, the rays are refracted by the drop to form a shadowgraphic image on a screen far from the drop, usually with an outmost bright thick ring and a set of fringes, as shown in Fig. 1a. The drop-refracting far-field shadowgraphic image can also show the inner convection flows, if any. Typical shadowgraphic images are shown in Figs. 1b and 1c, with and without convection flow in the drop, respectively. Both clearly show the bright thick ring and a set of fringes. Many investigators reported the fringes in the image and considered them to be the diffraction of laser light at the sharp edge of drop without an explanation of the outmost bright thick ring.[4,13,14] Actually, the explanation given by previous investigators for the fringes is incorrect. As is well known, a precursor film exists at the very edge of spreading drop front, whereas the macroscopic portion of the drop is shaped as a spheroid cap. A crossover region between the film and the macroscopic portion of the drop takes an asymptotic form. Evidently, spreading drops have no sharp edges. Instead, an inflexion line must exist on the drop surface, as shown in Fig. 1a. In reality, the outmost bright thick ring is the caustic line formed by the close-set rays passing through the drop at the inflexion line, whereas the fringes are the caustic diffraction, which is different from the diffraction given by the initial wave front edges cut off.[15] As pointed out by Nye,[16] the caustic diffraction arises from a lack of flatness in the initial wave front, rather than from the fact that it is bounded. In other words, it arises because the initial wave front itself starts out with a phase variation across it instead of the diffraction fringes coming from the edges of the aperture (the so-called aperture effect.) Besides, to explain the formation of the fringes correctly, it is more important use the information about the drop edge implied by the fringes.

According to the analysis by Berry,[15] caustic diffraction occurs in the far field of the wave as well, manifested by the fringes next to the caustics. As pointed out by Nye,[16] the most elementary way of treating the diffraction is in terms of interfering rays, known as the semiclassical approximation. Each ray is regarded as carrying an amplitude and a phase, so that they may interfere. Based on this approximation, the caustic diffraction can be considered a result produced by the interference between the rays at both side of the inflexion. The region around the inflexion line is the so-called protruding foot with a height of b, as shown in Fig. 1a. It can be seen from the details of area $\boldsymbol{A}$ in Fig. 2 that the wavefront with a point of inflexion Q produces a focusing effect in far field of the wave. The closely neighboring rays at both sides of point Q converge to the ray passing through point Q in the far field of the wave, at the inner side, to form a caustic line, the outmost bright thick ring. Meanwhile, the farther neighboring rays interfere with each other, as long

Received 16 February 2005; revision received 12 July 2005; accepted for publication 12 July 2005.

*Research Scientist, Mail Stop 77-5, Microgravity Division.
†Senior Scientist, Department of Workforce Enhancement; n.zhang@grc.nasa.gov.

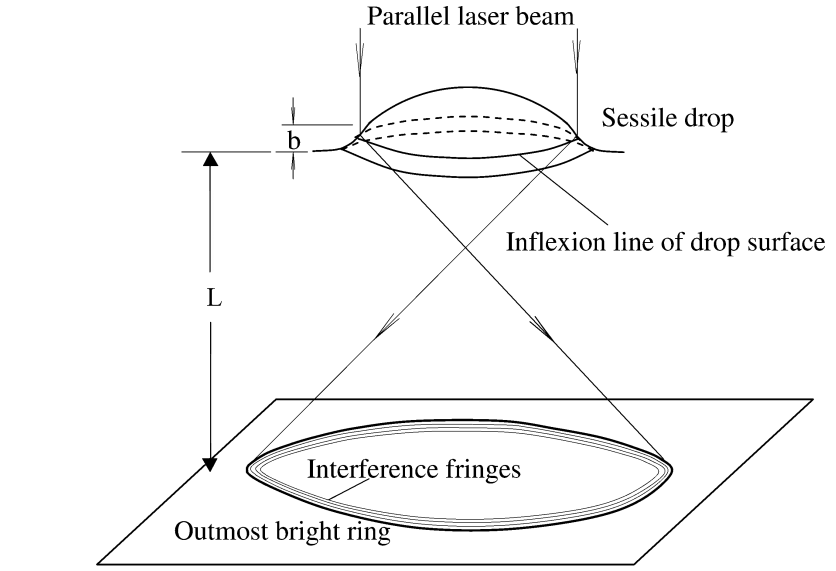

a)

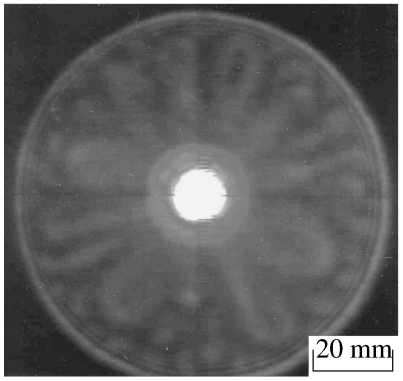

b)

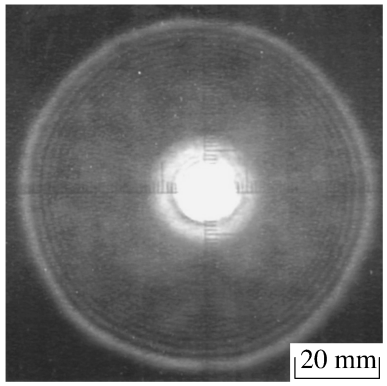

c)

Fig. 1 Shadowgraphic image of sessile drop on screen far from drop and typical shadowgraphic images of 5.0-μl drop with $L = 630.5$ mm: a) schematic of drop-refractive shadowgraph, b) R-113 drop at $\tau = 0.75$, and c) cyclohexane drop at $\tau = 0.60$.

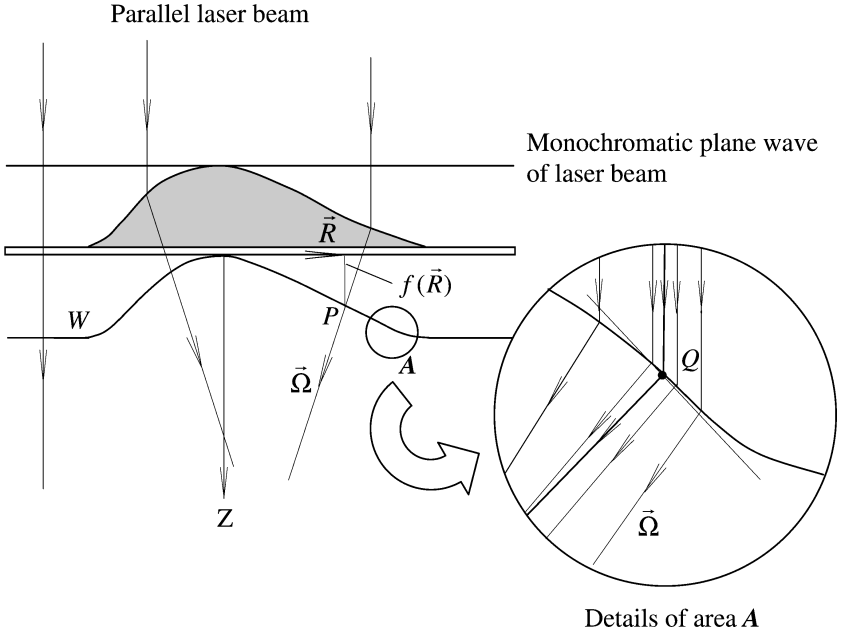

Fig. 2 Wave front deformed by refraction of sessile drop.

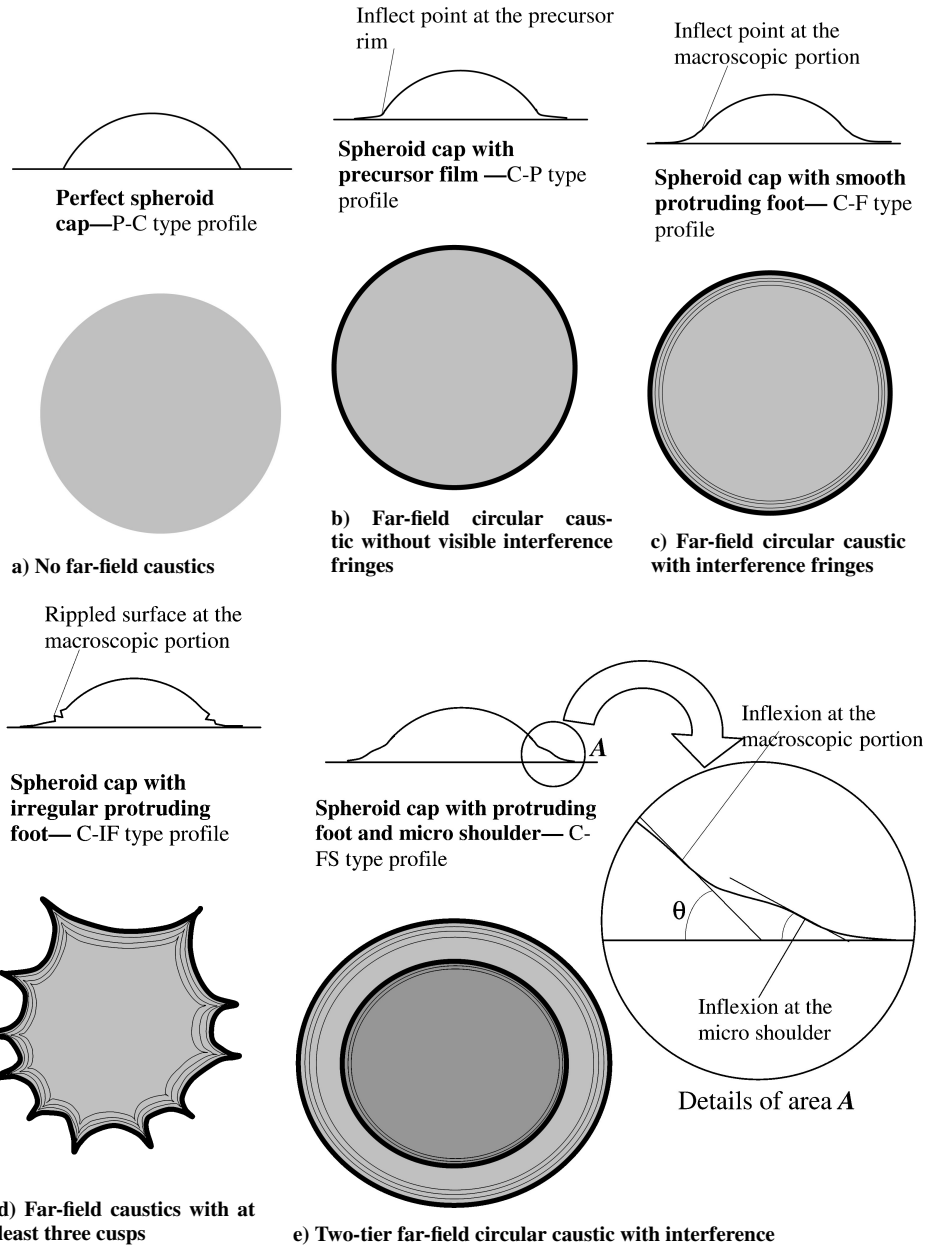

Fig. 3 Different drop profile patterns and their corresponding far-field shadowgraphic images.

as their optical-path differences are integer increments of the laser wavelength, to produce interference fringes. All of these fringes fall in the inner side of the caustic line, as shown in Fig. 1.

III. Experimental Results and Discussion

As shown in Fig. 3, there are five basic patterns of the spreading and evaporating drop profiles: 1) perfect spheroid cap (P-C type), 2) spheroid cap with precursor film (C-P type), 3)spheroid cap with smooth protruding foot (C-F type), 4) spheroid cap with irregular protruding foot (C-IF type), and 5) spheroid cap with a protruding foot and a microshoulder (C-FS type). The first four patterns were reported by Zhang and Chao.[9] This study further reveals that the first three patterns of the drop profile often appear in succession in the early stage of spreading. Experimental results show that, for common liquids, including highly wetting liquids, such as fluoroinert (FC-72) and refrigerant 113 (R-113), and moderately wetting liquids, such as water and ethanol, the sessile drops form a perfect spheroid cap (P-C-type profile) only at the very beginning of spreading when the drop has not yet spread. The fact that no bright ring appears on the images implies that the drop surfaces have no inflexion anywhere, and therefore, no crossover region exists. At this point, the drops have a perfect spheroid cap. When the drop starts spreading, a precursor film immediately forms on the solid surface. At the same time, an inflexion line around the drop occurs near the TPCL under the combined actions of interface tensions and viscosity resistance, where a crossover region forms to complete the transition from the macroscopic portion of the liquid body to the precursor film. When a parallel laser beam passes though the inflexion line and its close neighbor, a far-field caustic occurs. It is the caustic that forms the outmost bright thick ring on the far-field screen. This implies that the inflexion line immediately occurs after the drop starts spreading. Subsequently, the inflexion line migrates up to a certain position as the spreading develops, while the slope variation of the drop surface in the crossover region becomes relatively smaller.

During the fully developed stage of the spreading and evaporation process of a sessile drop, the liquid wetting and spreading properties fully emerge on the far-field shadowgraphic image. For stable spreading liquids, such as FC-72, R-113, cyclohexane, n-pentane, and chloroform, the drop maintains its smooth surface all of the way. Some liquid drops, for example, R-113 exhibit strong capillary flow from the very beginning to the end of the spreading and evaporation process without influence on the surface smoothness.[12] In some liquid drops, such as cyclohexane and chloroform, there

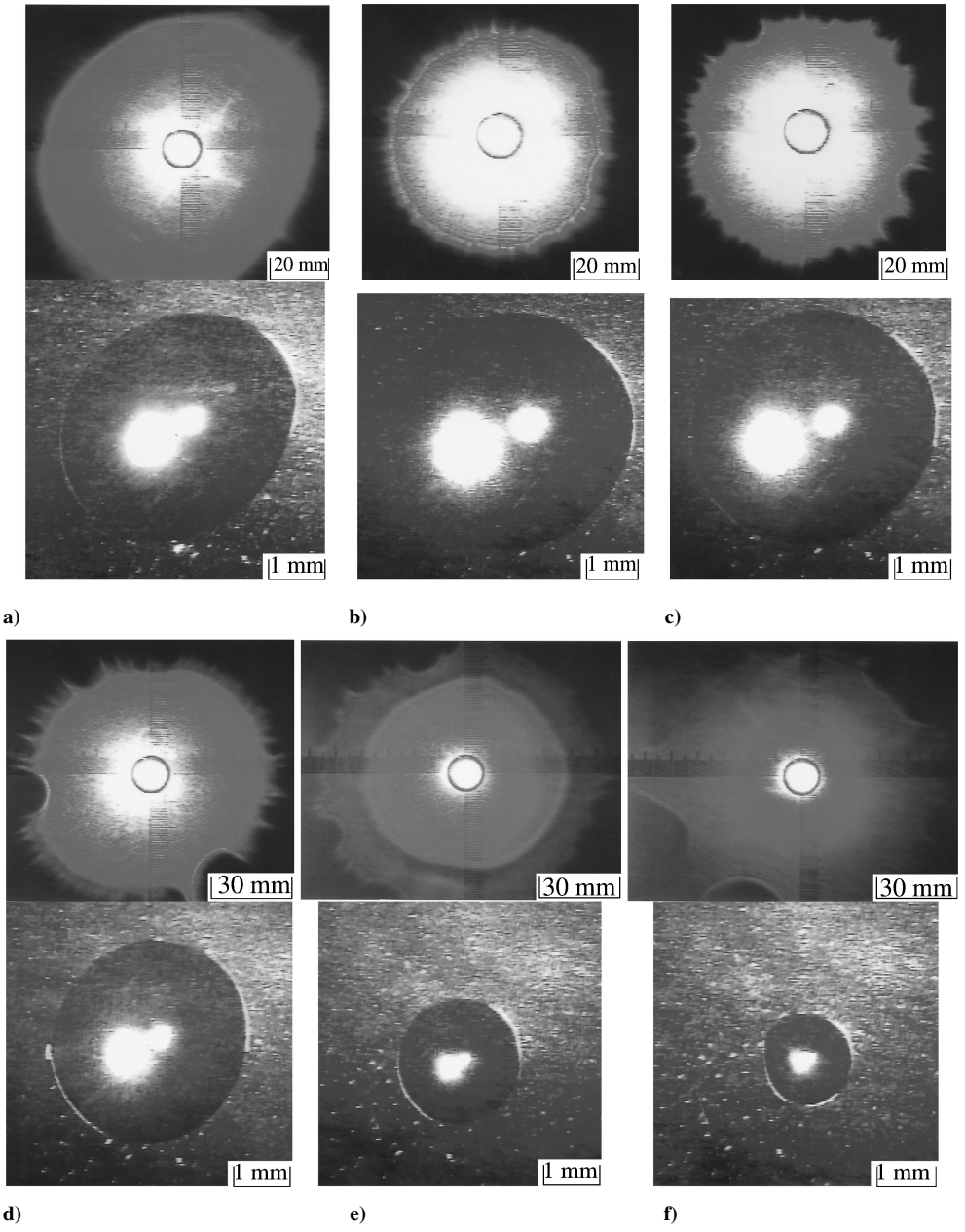

Fig. 4 Typical far-field shadowgraphic images with corresponding magnified top views of cyclohexene drop: a) at $\tau' = 1.022 \times 10^{-3}$, b) at $\tau' = 0.0291$, c) at $\tau' = 0.115$, d) at $\tau' = 0.325$, e) at $\tau' = 0.804$, and f) at $\tau' = 1.0$.

is no capillary flow at all from the beginning to the end. In others, for example, FC-72, the capillary flow occurs only at some time after the spreading starts and disappears before the drop dries. On the other hand, for the unstable spreading liquid drops, such as water, cyclohexene, ethanol, methanol, etc., the drop cannot retain its surface smoothness during the spreading and evaporating process. Usually, the instable spreading liquid drops have no capillary flow, but their surface smoothness varies considerably.

A new interesting profile pattern of a spreading drop is revealed in the cyclohexene drop spreading/evaporating process. As a cyclohexene drop of 2.14 μl spreading and evaporation takes place, its contact diameter continuously increases until $t = 1.9$ s and then decreases, as shown in Fig. 4. The far-field shadowgraphic images of the drop show typical unstable spreading. The caustic is nearly a smooth circle at the beginning, then becomes multithorned, implying that cusps on the caustic form and grow in number, as shown in Figs. 4a–4c. During the contact diameter contraction, a second caustic emerges on the far-field shadowgraphic image at $t = 21.17$ s, as shown in Fig. 4d. The second caustic is brighter and smooth on the inside. The original one with many cusps on the outside becomes dull, as shown in Figs. 4d and 4e. This implies that two inflexion lines exist near the TPCL region. The inner, smooth caustic is produced by a microshoulder close to the precursor film, whereas the outer caustic with cusps is formed by the beam passing though the inflexion line at the crossover region between the bulk body and the microportion of the drop, as shown in Fig. 3e. The inner caustic continuously contracts until disappearance at $t = 65.2$ s, implying the microshoulder migrates down and finally fades into the precursor. Once again, the far-field shadowgraphic images clearly show the subtle deformation of the drop surface through the caustic with many cusps, indicating drop-spreading instability that cannot be detected from the magnified top view of the drop shown in Fig. 4. On the other hand, the smooth inner caustic on the shadowgraphic image shown in Fig. 4e indicates that the drop surface at the microshoulder near the precursor film is smooth. The mechanism of formation of this profile pattern is not clear.

Because the lifetime of the cyclohexene sessile drop is relatively long, lasting several days in general, and both shadowgraphic image and top view of the drop have almost no change, the spreading and evaporation time when the inside caustic circle disappears is

taken as the eigenlifetime t'_f. This gives the dimensionless spreading and evaporation eigentime $\tau' \equiv t/t_{f'}$, which is used in the tests of cyclohexene drops, as shown in Fig. 4.

Note that the spreading of a cyclohexene drop is very sensitive to the surface condition. Different surface cleaning methods results in the cyclohexene drop having different spreading characteristics. For example, on slide glasses cleaned by hydrochloric acid or by flame cleaning, a cyclohexene drop spreads quickly to form a pancake within 0.3 s, showing typical complete wetting characteristics,[17] and then evaporates shortly thereafter. On the contrary, the spreading of FC-72 and R-113 drops on the slide glass is not at all influenced by the cleaning method. The same characteristics are observed for these drops on slide-glass surfaces cleaned by different methods. The mechanisms of surface-sensitive spreading of cyclohexene and the inertia spreading of FC-72 and R-113 have not yet been established, and more experimental, and theoretical work is needed to determine and verify those effects.

IV. Conclusions

The drop-refracting shadowgraphy method has been successfully used to identify the profiles of spreading drops. Five basic profile patterns are revealed through the analysis of caustics and caustic diffraction, based on wave theory. It was found that the three basic patterns, that is, perfect spheroid cap P-C type, spheroid cap with precursor film C-P type, and spheroid cap with smooth protruding foot C-F type, often appear in succession at the early stage of spreading. The P-C-type profile only occurs at the beginning of spreading. The pattern of the spheroid cap with an irregular protruding foot (C-IF type) expresses the instability of sessile drops. A particular pattern, spheroid cap with a protruding foot and a microshoulder (C-FS type), is found in the cyclohexene drop spreading and evaporation process.

The far-field shadowgraphic image of a sessile drop is sensitive to surface deformation, and for this reason, the drop-refracting-shadowgraphy setup is a powerful instrument for detecting the spreading instability of liquid drops.

References

[1]Leger, L., and Joanny, J. F., "Liquid Spreading," *Reports Progress in Physics*, Vol. 55, No. 4, 1992, pp. 431–486.

[2]Pompe, T., and Herminghaus, S., "Three-phase Contact Line Energetics from Nanoscale Liquid Surface Topographies," *Physical Review Letters*, Vol. 85, No. 9, 2000, pp. 1930–1933.

[3]de Gennes, P. G., "Wetting: Statics and Dynamics," *Reviews of Modern Physics*, Vol. 57, No. 3, 1985, pp. 827–863.

[4]Zhang, N., and Yang, W. J., "Natural Convection in Evaporating Minute Drops," *Journal of Heat Transfer*, Vol. 104, No. 2, 1983, pp. 656–662.

[5]Zhang, N., and Yang, W. J., "Evaporative Convection in Minute Drops on a Plate with Temperature Gradient," *International Journal of Heat and Mass Transfer*, Vol. 26, No. 10, 1983, pp. 1479–1487.

[6]Zhang, N., and Yang, W. J., "Microstructure of Flow Inside Minute Drops Evaporating on a Surface," *Journal of Heat Transfer*, Vol. 105, No. 4, 1983, pp. 908–910.

[7]Zhang, N., and Chao, D. F., "A New Approach to Measure Contact Angle and Evaporation Rate with Flow Visualization in a Sessile Drop," NASA TM-1999-209636, Dec. 1999.

[8]Zhang, N., and Chao, D. F., "Effects of Evaporation/Condensation on Spreading and Contact Angle of a Volatile Liquid Drop," *Heat Transfer Science and Technology 2000*, edited by B. X. Wang, High Education Press, Beijing, 2000, pp. 367–372.

[9]Chao, D. F., and Zhang, N., "Effects of Evaporation and Thermocapillary Convection on Volatile Liquid Droplets," *Journal of Thermophysics and Heat Transfer*, Vol. 15, No. 4, 2001, pp. 416–420.

[10]Zhang, N., and Chao, D. F., "Caustics and Caustic-diffraction in Laser Shadowgraphy of a Sessile Drop and Identification of Profile near Contact Line," *Optics and Laser Technology*, Vol. 35, No. 3, 2003, pp. 155–161.

[11]Zhang, N., and Chao, D. F., "Profile Measurement and Flow Visualization of Sessile Drop Through Laser Shadowgraph," *Proceedings of 7th International Symposium on Flow Control, Measurement and Visualization*, CD ROM Paper 185, Optimage Ltd., Edinburgh, 2003.

[12]Chao, D. F., Zhang, N., and Yang, W. J., "Profile at a Contact Line for Evaporating Sessile Drops and Visualization of Capillary Flow," *Journal Flow Visualization and Image Processing*, Vol. 10, No. 3-4, 2003, pp. 183–194.

[13]Tanner, L. H., "The Spreading of Silicone Oil Drops on Horizontal Surfaces," *Journal of Physics D: Applied Physics*, Vol. 12, No. 9, 1979, pp. 1473–1484.

[14]Allain, C., Ausserre, D., and Rondelez, F., "A New Method for Contact-angle Measurements of Sessile Drops," *Journal of Colloid Interface Science*, Vol. 107, No. 1, 1985, pp. 5–13.

[15]Berry, M. V., "Waves and Thom's Theorem," *Advances in Physics*, Vol. 25, No. 1, 1976, pp. 1–26.

[16]Nye, J. F., *Natural Focusing and Fine Structure of Light*, IOP Pub., Ltd., Bristol, England, U.K., 1999.

[17]Brochard-Wyart, F., di Meglio, J.-M., Quere, D., and de Gennes, P.-G., "Spreading of Nonvolatile Liquids in a Continuum Picture," *Langmuir*, Vol. 7, No. 2, 1991, pp. 335–338.